Radio Interferometric Studies of Cool Evolved Stellar Outflows

A dissertation submitted to the University of Dublin
for the degree of Doctor of Philosophy

Eamon O'Gorman

Supervisor: Dr. Graham M. Harper

Trinity College Dublin, September 2013

Declaration

I declare that this thesis has not been submitted as an exercise for a degree at this or any other university and it is entirely my own work.

I agree to deposit this thesis in the University's open access institutional repository or allow the library to do so on my behalf, subject to Irish Copyright Legislation and Trinity College Library conditions of use and acknowledgement.

Name: Your Name

Signature: .... **Date:** ....

Summary

You should write a nice summary here...

A dedication if you wish...

Acknowledgements

Some sincere acknowledgements...

List of Publications

Refereed

1. **O'Gorman, E.**, Harper, G. M., Brown, J. M., Brown, A., Redfield, S., Richter, M. J., and Requena-Torres, M. A.
   "CARMA CO(J = 2 - 1) Observations of the Circumstellar Envelope of Betelgeuse"
   The Astronomical Journal, 144, 36 (2012)

2. Sada, P. V., Deming, D., Jennings, D. E., Jackson, B. K., Hamilton, C. M., Fraine, J., Peterson, S. W., Haase, F., Bays, K., Lunsford, A., and **O'Gorman, E.**
   "Extrasolar Planet Transits Observed at Kitt Peak National Observatory"
   Publications of the Astronomical Society of the Pacific, 124, 212 (2012)

3. Sada, P. V., Deming, D., Jackson, B. K., Jennings, D. E., Peterson, S. W., Haase, F., Bays, K., **O'Gorman, E.**, and Lundsford, A.
   "Recent Transits of the Super-Earth Exoplanet GJ 1214b"
   The Astrophysical Journal Letters, 720, L215 (2010)

Non-Refereed

1. **O'Gorman, E.**, & Harper, G. M.
   "What is Heating Arcturus' Wind?",
   Proceedings of the 16th Cambridge Workshop on Cool Stars, Stellar Systems and the Sun. Astronomical Society of the Pacific Conference Series, 448, 691 (2011)

Contents

List of Figures

List of Tables

1
Introduction

Here is the introduction of the thesis, complete with a few references (Prothero & Buell, 2007; Sagan, 1997). Section 3.1 contains Equation 1.1, Section 3.2 has Figure 1.1 and Section 3.3 has Table 1.1. Chapter 2 has pretty much nothing in it.

1.1 First Section

This section has an equation. Here it is:

$$L_\odot = 4\pi R_\odot^2 \sigma T_e^4 \tag{1.1}$$

which is a nice way of describing the luminosity.

1.2 Second Section

So this section has a figure in it[1]. That figure depicts the basic structure of a red giant.

---

[1]And also a footnote.
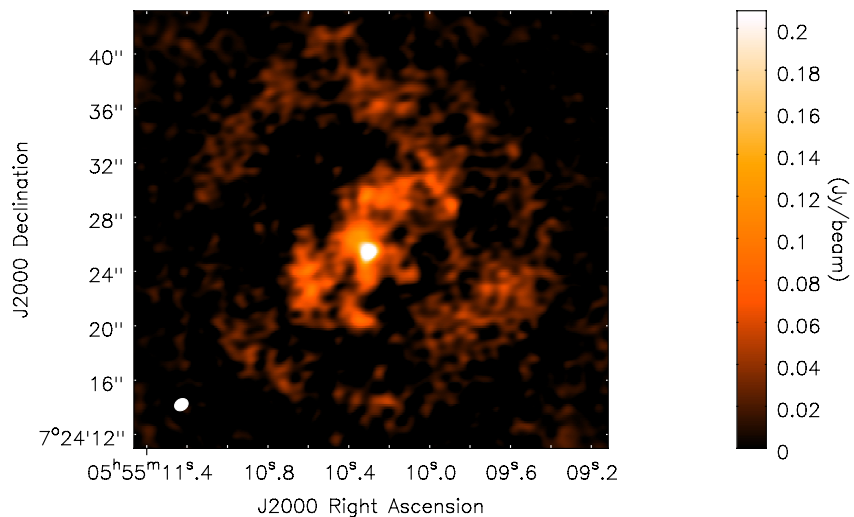
Figure 1.1: Red Giant and Asymptotic Giant Branch Stars. The left side of the figure shows the basic structure of a star on the giant branch of the HR diagram, while the right side shows a similar star after it has evolved to ascend the asymptotic giant branch. *Image Credit: Australian Telescope National Facility.*

1.3   Second Section

This section contains a basic table.

Table 1.1: Physical Properties of α Boo and α Tau.

Property	α Boo	α Tau	Reference
HD Number	124897	29139	. . .
Spectral Type	K2 III	K5 III	1, 2
ra (ICRS: ep=J2000)	$14^\mathrm{h}15^\mathrm{m}39.672^\mathrm{s}$	$04^\mathrm{h}35^\mathrm{m}55.239^\mathrm{s}$	3
dec (ICRS: ep=J2000)	$+19\ 10\ 56.673$	$+16\ 30\ 33.489$	3
pm-ra (mas yr^{-1})	-1093.39 ± 0.44	63.45 ± 0.84	3
pm-dec (mas yr^{-1})	-2000.06 ± 0.39	-188.94 ± 0.65	3
π (mas)	88.83 ± 0.54	48.94 ± 0.77	3
Distance (pc)	11.3±0.1	20.4±0.3	3
M ($M_\odot$)	0.8±0.2	1.3±0.3	6, 4
θ_UD (mas)	21.0±0.2	20.2±0.3	5
θ_LD (mas)	21.0±0.2	20.2±0.3	5
L ($L_\odot$)			
R ($R_\odot$)	25.4±0.3	44.4±1.0	. . .
Log g			
T_eff (K)	4294±30	3970±49	5
v_rad (km s^{-1})	$+5.19 \pm 0.04$	$+54.11 \pm 0.04$	9
v_esc (km s^{-1})	110	106	. . .
v_∞ (km s^{-1})	∼40	∼30	7, 8
T_wind (K)	∼10,000	<10,000	7, 8
$\dot{M}$ ($M_\odot$ yr^{-1})	2×10^{-10}	1.6×10^{-11}	7, 8
H ($H_\odot$)			. . .
Fe/H	-0.5±0.2	0.00±0.2	10

References.-(1);(2)Gray *et al.* (2006); (3)van Leeuwen (2007); (5)di Benedetto (1993); (6)Kallinger *et al.* (2010); (7)Drake (1985); (8)Robinson *et al.* (1998) (9)Massarotti *et al.* (2008); (10)Decin *et al.* (2003)

2

Introduction to Radio Interferometry

The poor spatial resolution provided by a single dish radio antenna can cause difficulties in obtaining accurate flux density measurements of radio astronomical sources, especially at long wavelengths. A single dish radio antenna is unable to distinguish against background radio emitters located in the primary beam, and therefore the the observed flux density can contain emission from unrelated sources. This limitation can be overcome through interferometry. An interferometer acts as a spatial filter, and can discriminate against smooth backgrounds while its higher resolution allows seperation of the target from nearby confusing sources.

2.1 Radio Antenna Basics

The quality and properties of the final radio image produced from a synthesis array are partially dependent on the properties of the the individual antennae in the array. The most important such properties are discussed in the following sections and include aperture size, aperture efficiency, pointing accuracy, sidelobe level and noise temperature. We define the radio antenna as the piece of equipment which converts the electromagnetic waves emitted from the observed source into

an electric current ready to be input into to the first low noise amplifier where the signal is at the radio/sky frequency, ν_{RF}.

2.1.1 Radio Antenna Formulae

The power gain of a transmitting antenna is a measure of the antenna's capability of converting power into radio waves in a specific direction. In radio astronomy, the receiving counterpart of transmitting power gain is the effective collecting area of an antenna, $A(\nu,\theta,\phi)$, where ν is frequency and θ and ϕ are direction coordinates. An ideal radio antenna would collect all incident radiation from a distant point source and convert it to electrical power. The total spectral power P_ν, collected by it would then be a product of its geometric area and the incident spectral power per area, or flux density F_ν. By analogy then, the effective area of a real radio antenna is defined

$$A(\nu, \theta, \phi) = \frac{P_\nu}{F_\nu} = \frac{P}{I(\nu, \theta, \phi)\Delta\nu\Delta\Omega} \tag{2.1}$$

where $I(\nu,\theta,\phi)$ is the source brightness in units W m^{-2} Hz^{-1} sr^{-1} that the antenna is pointing at and P is the power (in Watts) received by the antenna in bandwidth $\Delta\nu$ from element $\Delta\Omega$ of solid angle. The normalized antenna reception pattern $\mathcal{A}$, often referred to as the power pattern due to the duality between receiving and transmitting, is defined as

$$\mathcal{A}(\nu, \theta, \phi) = \frac{A(\nu, \theta, \phi)}{A_0} \tag{2.2}$$

where A_0 (m^2) is often referred to as the effective area of the antenna and is the response at the center of the main lobe of $A(\nu,\theta,\phi)$ [i.e. A$(\nu,0,0)$]. Then the beam solid angle, Ω_A, of the primary beam is

$$\Omega_A = \iint_{\text{all sky}} \mathcal{A}(\theta, \phi)d\Omega \tag{2.3}$$

and is a measure of the field of view of the antenna.

In the case of an isotropic antenna [i.e., $\mathcal{A}(\nu, \theta, \phi) = 1$], it can be shown that the product of the effective area and the primary beam solid angle is equal to the

square of the wavelength (Kraus *et al.*, 1986)

$$A_0 \Omega_A = \lambda^2. \tag{2.4}$$

Ω_A has its maximum possible value of 4π if $\mathcal{A}$ is everywhere equal to 1. This means that the primary antenna can see the whole sky with equal sensitivity. Even though a large field of view is usually desirable in radio astronomy, Equation 2.4 ensures that for any given wavelength, when Ω_A is a maximum, the power received is a minimum and therefore the sensitivity is also at a minimum. To improve sensitivity, one could increase the collecting area of the antenna, but Equation 2.4 then ensures that the field of view must decrease. Thus, when deciding on the primary antenna size in a synthesis array, there is always a trade-off between field of view and sensitivity.

In reality, an antenna cannot radiate isotroptically and will radiate preferentially in one or more directions. A Fourier transform relationship exists between the complex voltage distribution of the field, $f(u,v)$, in the aperture of the antenna and the complex far-field voltage radiation pattern, $F(l,m)$, of the antenna (Kraus *et al.*, 1986)

$$F(l,m) = \iint_{\text{aperture}} f(u,v) e^{2\pi i (ul+vm)} du dv \tag{2.5}$$

and

$$f(u,v) = \int_{\infty}^{\infty} \int_{\infty}^{\infty} F(l,m) e^{-2\pi i (ul+vm)} dl dm \tag{2.6}$$

where

$$u = \sin\theta\cos\phi \quad \text{and} \quad v = \sin\theta\sin\phi \tag{2.7}$$

are the antenna coordinates and l and m are their Fourrier counterparts. The from of $f(u,v)$ is determined by the manner in which the antenna feed illuminates the aperture. Therefore Equations 2.6 and 2.7 tell us that the radiation pattern in the far-field of a two-dimensional aperture is the two-dimensional Fourier transform of the aperture field illumination. For a uniformly illuminated 1-D aperture shown in Figure x, the radiation pattern in the far-field is the *sinc* function. The radiation pattern in the far-field, $F(l,m)$, of such an antenna is related to the antenna power pattern, $\mathcal{A}$, by $\mathcal{A} = |F(l,m)|^2$. This power pattern is known as the Airy pattern

if the antenna is uniformly illuminated and is also shown in Figure x. The central peak of this power pattern is called the main beam while the smaller secondary peaks are called sidelobes. The antenna is maximally sensitive to radiation from the direction of the peak of the beam, but is also slightly sensitive to radiation in the direction of the side lobes. The half-power beamwidth (HPBW) of the main beam, θ_{HPBW}, is a term commonly used in the literature to describe the field of view of an antenna/interferometer and satisfies

$$\theta_{\mathrm{HPBW}} \propto \frac{\lambda}{D} \tag{2.8}$$

where D is the diameter of the antenna. The constant of proportionality varies slightly with the illumination taper and is $\sim 0.9 - 1.2$ for most single-dish radio antennae.

Figure

Maybe mention resolution? I.e. Rayleigh criteria

2.1.2 Antenna Structural Design

The design of the primary antenna element of an interferometric array will depend on the wavelength range to be observed. In general, wire antennas are used for wavelengths longer than ~ 1 m, while reflector antennas are typically used at shorter wavelengths. The reason why the more simple and less expensive wire antennas are not used at all wavelengths is given by Equation 2.4. For an isotropic antenna, this equation tells us that the effective area is just

$$A_0 = \frac{\lambda^2}{4\pi}. \tag{2.9}$$

Therefore, at short wavelengths a non-directional antenna such as a dipole, will have a small effective collecting area, giving it poor sensitivity for reception. Thus, wire antennas can be used at long wavelengths as they have sufficient collecting area, but cannot be used at shorter wavelengths as an impractical amount would be needed to produce useful collecting areas. Since the interferometric arrays used in this thesis use reflector antennas, the rest of this section will focus on them.

Choice of Antenna Mount. Nearly all interferometric arrays consist of antennas which have altitude over azimuth (altazimuth) mounts. These antennas lie on a horizontal azimuth track on which the antenna can turn in azimuth, and a horizontal elevation axle about which the antenna changes in zenith angle. The main advantage of such a design is simplicity and thus lower cost. Gravity always acts on the reflector in the same plan thus reducing the problem of keeping the reflector profile accurate during the duration an observation. However, sources close to the zenith cannot be observed due to the high rate of azimuth rotation required. Also, the beam rotates with respect to the source for long duration observations which can affect the dynamic range of total intensity images of very large sources. The other type of mount occasionally used is the equatorial mount. Its polar axis is aligned parallel to the axis of rotation of the Earth and therefore only needs to rotate about the declination axis to observe a source. Its beam also doesn't have the beam rotation problem encountered by the altazimuth design and can track sources close to the zenith. Its major disadvantage and the reason for its scarce usage is the complexity of its design and resulting increased cost.

Choice of Antenna Optics. In Figure x(say adopted from Synthesis Imaging) we show the main optical systems which can be used to feed a large radio reflector (). The prime focus system (e.g. used in the Giant Meter Radio Telescope) has the advantage that it can be used at long wavelengths where the use of secondary focus feeds (i.e. sub-reflectors) become impractical. However, access to, and space for, the feed and receiver is limited and sensitivity can be lost due to spillover noise from the ground. The other designs have the advantage of easier access to the feeds and receivers and less spillover noise from the ground. The off-axis Cassegrain (e.g. used in the Very Large Array) has also the advantage of increased frequency capability as many feeds can be located in a circle around the centre of the reflector and a slight rotation of the sub-reflector is all that is required to change observing frequency. The receivers and feeds in the Naysmith geometry (e.g used in the Combined Array for Research in Millimeter wave Astronomy) are located externally to the antenna structure. Finally, the offset Cassegrain (e.g. planned to be implemented on the Square Kilometer Array

antennas) has no blockage and will have a circularly symmetric beam with low sidelobes but the increase complexity of its structure leads to increased costs.

2.1.3 Antenna Performance Parameters

Aperture Efficiency. The geometric collecting area of a parabolic antenna, A_{geo} $[= \pi(D/2)^2]$, is related to the effective area (i.e. the collecting area when pointing directly at a source) via the dimensionless quantity, η, known as the aperature efficiency where

$$\eta = \frac{A_0}{A_{\mathrm{geo}}} \qquad (2.10)$$

and is always less than unity. The aperture efficiency directly impacts on the sensitivity of the interferometric array and can be defined as the product of a number of different efficiency loss factors,

$$\eta = \eta_{\mathrm{sf}}\eta_{\mathrm{bl}}\eta_{\mathrm{s}}\eta_{\mathrm{t}}\eta_{\mathrm{misc}}. \qquad (2.11)$$

The surface efficiency, η_{sf}, accounts for the aperture efficiency loss as a result of reflector profile inaccuracies. Such inaccuracies result in the electric field from various parts of the aperture not adding together in phase at the feed leading to a decrease in power. The aperture blockage efficiency, η_{bl}, accounts for the fact that the subreflector (or feed) and its support structure result in a reduction in the incident radiation on the antenna. The feed spillover efficiency, η_{bl}, is best understood if the antenna is considered in transmission rather than in reception mode, and is defined as the fraction of power radiated by the feed that is intercepted by the reflector for a prime focus system, or by the subreflector for a Cassigrain system. The illumination taper efficiency, η_{t}, accounts for the fact that the feed pattern does not illuminate the primary reflector uniformly but illuminates the outer part of the reflector at a lower level than the inner part. Finally, the miscellaneous efficiency losses such as reflector diffraction and feed position phase errors are accounted for in η_{misc}.

Pointing Accuracy.

2.2 Fundamentals of Astronomical Interferometry

Young's Slits

2.3 The Synthesis Telescope

2.4 The Measurement Equation

3
Instrumentation and Observations

So this Chapter has nothing really, apart from a shout out to Appendix A, and maybe a few more sample references (Harper & Brown, 2006; Seaquist & Taylor, 1990).

3.1   CARMA

3.1.1   The Basic Instrument

3.1.2   The CARMA Electronic System

3.1.3   Observations

3.2   VLA

3.2.1   The Basic Instrument

3.2.2   The VLA Electronic System

3.2.3   Observation Preparation

3.2.4   Observations

3.3   GMRT

A A Nice Appendix

This is where the appendix would go...

References

Decin, L., Vandenbussche, B., Waelkens, C., Decin, G., Eriksson, K., Gustafsson, B., Plez, B. & Sauval, A.J. (2003). ISO-SWS calibration and the accurate modelling of cool-star atmospheres. IV. G9 to M2 stars. *Astronomy & Astrophysics*, **400**, 709–727. (Cited on page 3.)

di Benedetto, G.P. (1993). Empirical effective temperatures and angular diameters of stars cooler than the sun. *Astronomy & Astrophysics*, **270**, 315–334. (Cited on page 3.)

Drake, S.A. (1985). Modeling lines formed in the expanding chromospheres of red giants. In J.E. Beckman & L. Crivellari, eds., *Progress in stellar spectral line formation theory; Proceedings of the Advanced Research Workshop, Trieste, Italy, September 4-7, 1984 (A86-37976 17-90). Dordrecht, D. Reidel Publishing Co., 1985, p. 351-357.*, 351–357. (Cited on page 3.)

Gray, R.O., Corbally, C.J., Garrison, R.F., McFadden, M.T., Bubar, E.J., Mc-Gahee, C.E., O'Donoghue, A.A. & Knox, E.R. (2006). Contributions to the Nearby Stars (NStars) Project: Spectroscopy of Stars Earlier than M0 within 40 pc-The Southern Sample. *Astronomical Journal*, **132**, 161–170. (Cited on page 3.)

Harper, G.M. & Brown, A. (2006). Electron Density and Turbulence Gradients within the Extended Atmosphere of the M Supergiant Betelgeuse (α Orionis). *Astrophysical Journal*, **646**, 1179–1202. (Cited on page 11.)

Kallinger, T., Weiss, W.W., Barban, C., Baudin, F., Cameron, C., Carrier, F., De Ridder, J., Goupil, M.J., Gruberbauer, M., Hatzes, A., Hekker, S., Samadi, R. & Deleuil, M. (2010). Oscillating red giants in the CoRoT exofield: asteroseismic mass and radius determination. *Astronomy & Astrophysics*, **509**, A77. (Cited on page 3.)

Kraus, J.D., Tiuri, M., Raisanen, A.V. & Carr, T.D. (1986). *Radio astronomy receivers*. (Cited on page 6.)

Massarotti, A., Latham, D.W., Stefanik, R.P. & Fogel, J. (2008). Rotational and Radial Velocities for a Sample of 761 HIPPARCOS Giants and the Role of Binarity. *Astronomical Journal*, **135**, 209–231. (Cited on page 3.)

Prothero, D. & Buell, C. (2007). *Evolution: what the fossils say and why it matters.* Columbia University Press. (Cited on page 1.)

Robinson, R.D., Carpenter, K.G. & Brown, A. (1998). Goddard High-Resolution Spectrograph Observations of Cool Low-Gravity Stars. IV. A Comparison of the K5 III Stars alpha Tauri and gamma Draconis. *Astrophysical Journal*, **503**, 396. (Cited on page 3.)

SAGAN, C. (1997). *The Demon-Haunted World: Science as a Candle in the Dark*. Ballantine Books. (Cited on page 1.)

SEAQUIST, E.R. & TAYLOR, A.R. (1990). The collective radio properties of symbiotic stars. *Astrophysical Journal*, **349**, 313–327. (Cited on page 11.)

VAN LEEUWEN, F. (2007). Validation of the new Hipparcos reduction. *Astronomy & Astrophysics*, **474**, 653–664. (Cited on page 3.)